BALLOON-BORNE THREE-METER TELESCOPE FOR FAR-INFRARED AND SUBMILLIMETER ASTRONOMY

Grant NAGW-509

Semiannual Status Report No. 5

For the period 1 September 1985 through 28 February 1986

Principal Investigator

Dr. Giovanni G. Fazio

April 1986

Prepared for
National Aeronautics and Space Administration
Washington, D.C. 20546

Smithsonian Institution
Astrophysical Observatory
Cambridge, Massachusetts 02138

The Smithsonian Astrophysical Observatory
is a member of the
Harvard-Smithsonian Center for Astrophysics

The NASA Technical Officer for this grant is Dr. Nancy Boggess, Code EZ-7, National Aeronautics and Space Administration, Washington, D.C. 20546

BALLOON-BORNE THREE-METER TELESCOPE FOR FAR-INFRARED AND SUBMILLIMETER ASTRONOMY

Grant NAGW-509

Semiannual Status Report No. 5

For the period 1 September 1985 through 28 February 1986

Principal Investigator

Dr. Giovanni G. Fazio

April 1986

Prepared for
National Aeronautics and Space Administration
Washington, D.C. 20546

Smithsonian Institution
Astrophysical Observatory
Cambridge, Massachusetts 02138

The Smithsonian Astrophysical Observatory
is a member of the
Harvard-Smithsonian Center for Astrophysics

The NASA Technical Officer for this grant is Dr. Nancy Boggess, Code EZ-7, National Aeronautics and Space Administration, Washington, D.C. 20546

CONTENTS

1.0 INTRODUCTION

This is the fifth Semiannual Report submitted under Grant NAGW-509 for the development of a Balloon-Borne Three-Meter Telescope for Far-Infrared and Submillimeter Astronomy. It covers the period 1 September 1985 through 28 February 1986.

The Three-Meter Balloon Borne Telescope is a joint program of the Smithsonian Astrophysical Observatory (SAO), the University of Arizona and the University of Chicago. Under the terms of the Memorandum of Understanding for this program, SAO is responsible for program management and for providing the gondola structure with the attitude control and aspect systems, mechanical systems and telemetry and command systems; Arizona is responsible for optical design and fabrication and Chicago is responsible for determining focal-plane instrumentation requirements. SAO and Arizona share responsibility for the ground support data and control computer system.

Effort at SAO and Chicago during this reporting period focused on engineering evaluation of telescope gimbal designs. Arizona continued its mirror development and test program using mirror test blanks from Dornier and other sources under separate funding and will report on its effort independently. SAO, Arizona, and Chicago met by telephone conference during this period to coordinate activity and discuss technical issues.

2.0 SUMMARY OF WORK PERFORMED DURING REPORTING PERIOD

2.1 Introduction

A telescope bearing comparative study was done last year* as part of an optimization of predicted telescope pointing performance. The flex pivot was selected as the candidate bearing because:

1) It is frictionless;

2) It does not require a large support system (e.g., as an air bearing with its compressor);

3) It does not release condensible vapors (such as hydraulic oil) which are a hazard to the telescope optics.

A preliminary mechanical design of a gimbal was done during this reporting period based on the initial gimbal concept. We also talked to engineers at SAO who developed a flex-pivot-based gimbal system for a balloon spectrometer instrument and discussed their test results with them. Problems with the flex pivot design became apparent. Its limited rotation makes it cumbersome as an element in a gimbal system with a large angular range and precise alignment of the flex pivots on opposite sides of the gimbal is essential to achieving the desired performance. In light of this, ball bearings have now been re-examined for use as the main bearing elements.

---

*Fourth Semiannual Progress Report under this grant (NAGW-509) "Balloon-Borne Three-Meter Telescope for Far-Infrared and Submillimeter Astronomy", October 1985.

In this report we review the drawbacks we uncovered in the initial gimbal design, review the behavior of ball bearings in this application and propose two candidate gimbal designs which overcome the problems in the initial flex-pivot-based design.

2.2 Flex-Pivot-Based Design

2.2.1 Requirements -

The telescope gimbal and pointing control system design is driven by several requirements:

1) It must be able to track objects for one hour (i.e., 15° at the sidereal rate) with 1 arcsec RMS pointing accuracy;

2) It must be able to point the telescope to any azimuth angle in a 360° circle and any elevation angle from the horizon to the balloon obscuration angle ($\sim 67.5^{\circ}$).

3) It must be able to place the telescope vertically during launch and recovery operations for maximum protection of the optics.

The 15-degree range of uncompensated sidereal rotation places heavy demands on the flex pivot. It must support the telescope weight, have a low linear spring rate and have a reasonable fatigue cycle life ($> 10^4$) . A coarse positioning system is also required for telescope celestial pointing in the elevation axis.

2.2.2 Preliminary Design -

The preliminary gimbal designed to achieve these requirements consisted of two 6" diameter flex pivots, each with a large spring constant, and a flex pivot recentering system. The recentering system was envisioned as a standard worm and wheel acting on the gondola side of the flex pivot. When necessary the system would be automatically activated to unwind the flex pivot. During a slew or coarse pointing maneuver a lock would be engaged across the flex pivot to transfer the torque developed in the slewing maneuver across the gimbal and protect the flex pivot from being overstressed. Slew maneuvers would be carried out while the fine control loop was disabled. The gimbal lock prevented free mass/spring oscillations from occurring across the flex pivot.

2.2.3 Design Drawbacks -

The recentering system was a concern for several reasons:

1) It was another system which had to work to achieve a successful mission;

2) Its effect on telescope stability, if it activated during tracking, was unclear;

3) Its locking mechanism was an operational risk; it could fail while latched, shutting down the mission.

Problems related to flex pivot hysteresis were discovered on another SAO project. Hysteresis effects of the order of an arcminute were observed in that application. Controlling this source of

hysteresis and keeping its effect as low as possible require the gimbals to be coplanar and concentric to approximately 1 arcmin and 0.001 inch, respectively. Achieving this is not possible for all telescope load orientations in this telescope application.

2.2.4 Remedial Action -

In light of the design complications and hysteresis concerns related to the use of flex pivots, ball bearings were re-examined as the possible fine control bearing element. It was felt that many of the complications encountered in the flex pivot design would be eliminated.

2.3 Review of Ball Bearing Characteristics

2.3.1 Review Approach -

In order to compare the pointing precision of a gimbal system using ball bearings with one using flex pivots, some ball bearing characteristics must first be established. To do this, a general ball bearing size was selected and the bearing behavior was calculated under the known load conditions. The calculations drew heavily from the SAO Multiple Mirror Telescope (MMT) design experience and particularly on documentation by Philco/Ford from that program regarding azimuth drive bearing selection.

2.3.2 Results -

This review showed the following things:

1) The baseline bearing torque in this telescope is projected to be between 0.2-0.5 Nm. This is the normal load times the coefficient of friction acting at the bearing radius (i.e., $T_F = W_t . \mu . r_b$).

2) Another important friction torque contribution comes from the bearing's tendency to wobble. If the bearing is constrained, the wobble will produce a cyclic frictional torque which adds to the basic torque mentioned above. The phenomena of bearing wobble is not well understood. Thus it is hard to quantify the torque resulting from this effect. An estimate of its torque contribution could be as high as 1.5 Nm in this application.

3) Bearings in general exhibit a ± 10% variation in all sources of torque while rotating.

If the only bearing effect on the controllability of the system were the ± 10% variation in baseline torque, the ball bearing would yield an acceptable gimbal design. This variation, when treated as torque noise in the control models, yields a predicted pointing performance of better than ± 1 arcsec rms where only tracking velocity (angular rate) is controlled. Unfortunately, we must control the tracking position of the telescope and thus must take twice the prevailing bearing torque as the noise to the control system. This is at its lowest 0.4 Nm, much too great to overpower and still control

the pointing to better than 1 arcsec. We dealt with this problem earlier by using flex pivots during fine pointing operations and holding the main bearings fixed; now we want to look at how to overcome this bearing noise problem directly and eliminate the flex pivots from the main load bearing path.

2.4 A Proposed Design

2.4.1 Conceptual Approach -

A concept that utilizes the unlimited rotation of the ball bearing yet removes its friction losses is proposed. This consists of a ball bearing mounted directly to the telescope. The stationary side of the bearing (i.e., the gondola side) is mounted to a torque sensor. The measured torque indicated by the sensor is the frictional losses developed in the bearing (if the bearing were perfect, there would be no torque measured at its stationary side). This torque signal is fed to a torque motor which crosses the gimbal. Its stator is mounted to the gondola and its rotor to the telescope. The motor develops an equal and opposite torque to the measured torque and thereby counters the effect of the bearing noise on the telescope. The gimbal remains in a zero torque condition with respect to the gondola and telescope.

2.4.2 Requirements of a Successful Design -

In order to succeed this gimbal design must conform to a number of specified and derived design requirements:

1) The torque sensor must be capable of supporting the weight of the telescope in all orientations;

2) The sensor must have sufficient sensitivity to measure torques to a tenth of the maximum permissible noise torque (~.1 Nm);

3) The sensor must have a fast response (< 1ms);

4) The torque sensor must have a low enough spring constant to permit some motion of the telescope while the ball bearing is held up by friction. Thus for short ranges it must act like a flex pivot;

5) The torque motor must have a linear current/torque relationship or at least one which can be characterized and is time invariant;

6) The friction-like magnetic losses of the torquer must be low;

7) The whole gimbal must be stiff enough orthogonal to the gimbal axis to stay aligned.

2.4.3 Candidate Designs -

Several candidate designs have been discussed, but they limit themselves to two classes:

1) Use a flexure or flex pivot at the output side of the bearing. This would be instrumented with a strain gauge to determine torque and be calibrated and characterized to fully specify its behavior. There is some development risk associated with this method, but it has been done before.

2) Purchase or design a torque sensor that is capable of supporting the 1000 pound load yet is sensitive enough to yield the torque measurement. There are instruments like this available on the market.

Upon review both approaches appear to be viable. No decision has been reached on the method to employ.

2.5 System Controllability and Characteristics

2.5.1 Full System Model -

A nonlinear system block diagram is shown in Figure 1. This is quite similar to the Figure 2.4-3 on page 53 of the Preliminary Design Report*. The notable differences are the inclusion of the ball bearing in the flex pivot/ball bearing block, the ball bearing deflection, $\Delta \Theta_{Bi}$; its accumulation shown as $\Sigma \Delta \Theta_{Bi}$; and

*Fourth Semiannual Progress Report under this grant (NAGW-509) "Balloon-Borne Three-Meter Telescope for Far-Infrared and Submillimeter Astronomy", October 1985.

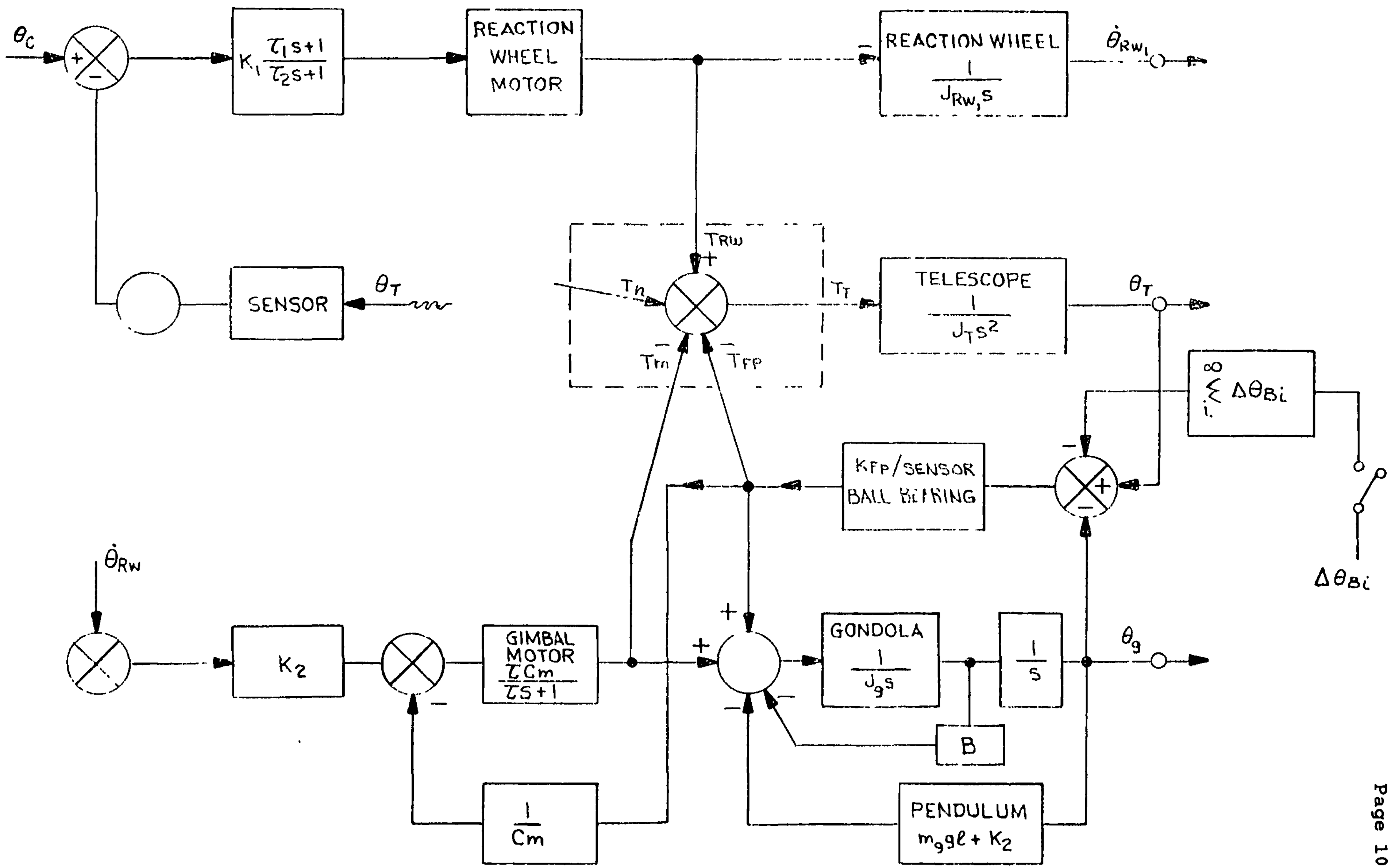

FIG. 1. SYSTEM BLOCK DIAGRAM

the explicit representation of the gimbal motor's time constant. The nature of the ball bearing deflection, which acts to reduce the quantity $(\Theta_T - \Theta_g)$, and thus the torque across the ball bearing and sensor, is not clearly definable. It must be assumed to be nonlinear and therefore beyond the capabilities of our present computer modelling program. Linear modelling does provide interesting results, though.

2.5.2 The Linear Model Configuration -

The telescope motion for most system operations will be absorbed by the torque sensor. The torque sensor will act as a flexure since, for small angles, the ball bearing will be locked by friction. When the stored torque in the flexure is equal to the bearing baseline friction, the ball bearing will rotate. There are many scenarios for the ball bearing behavior at the time of release but the worst case is a snap which centers the flex pivot (i.e., to zero torque). That this is the worst case can be seen by the following scenario: If the bearing were to relieve slowly the torque sensor would follow the relaxation and demand less torque from the gimbal motor. Ideally this would be transparent to the telescope as the gimbal motor would always track the bearing torque. However, if the bearing snapped back to the torque sensor's center point, the torque sensor and motor would not have time to follow and the net torque on the telescope and gondola would be that applied by the motor. The motor torque would decay to zero as the sensor reading and motor driver electronics overcome the motor time constant, T_m. However, the telescope would still have been subjected to a torque pulse approximately .2-.5 Nm in height and about

10 ms (4X the motor time constant) in duration.

A linear model can be constructed from these assumptions. It yields a simulation of the pointing system from which worst case performance can be judged. In that model the telescope is suspended on a flex pivot, has two controlled torque sources, the reaction wheel and the gimbal or ancillary motor, and yet is subjected to occasional noise pulses of $5x10^{-3}$ Nms that model the ball bearing snap. Assurance that this is a worst case system model will have to await the results of the simulation. This will obviously not predict limit cycle or other characteristic nonlinear behavior.

2.5.3 Possible Nonlinear Model -

In a nonlinear model the pivot/sensor torque would be compared to the breakfree frictional torque of the bearing. When these torques were equal the nonlinear representation of the bearing motion would be triggered. This activity would take place at the $\Delta\ \Theta_{B1}$ node in the block diagram representation of the system depicted in Figure 1. The torque felt by the telescope would be given by the time-dependent equation:

$$T(t) = \Delta\ \Theta_{B1}(t) . K_{FP/S}$$

for as long as the ball bearing deflected. The exact nature of the model nonlinearity (as opposed to the true system nonlinearity) would be twofold:

1) The comparator operation between the sensor torque and the breakfree frictional torque when it results in the switch (i.e., the bearing breaks away; and its symmetric operation to freeze the bearing motion); and

2) The nature of the function $\Delta \Theta_{Bi}(t)$.

However, the rest of the model and the equations will be the same as the linear representation. The nonlinearity will only present itself when the telescope has moved sufficiently to cause the flexure or sensor to develop a torque equal to that of the bearing breakfree. The required angle for breakfree torque is about 1°. This depends on the sensor spring constant and the bearing properties. The telescope's prime operation will be tracking stars, which will be rotating at 15°/hr. In their operation the nonlinearity will be excited on the order of every 4 minutes, very infrequent when compared to the control bandwidth of 2 Hz.

The linear model will not show any limit cycle behavior which might result from the bearing's stiction, however, we can determine if a limit cycle may result by looking at the system response to the bearing noise pulse. If the telescope motion is large it may excite a further bearing release (not shown by the linear model) and thus enter a limit cycle. If the predicted motion is small this will not be a problem. The linear simulation will indicate whether this is a problem area.

2.6 Development of System Equations

For the development of the linear equations please refer to Appendix B of the Preliminary Design Report, which is reproduced here as Appendix A. Referring to page 15 of the appendix we see that under the new system model the figure of the torque summing junction is still valid and the same as that shown here (in Figure 1 in dashed enclosure). In fact equations (1)+(2) of the appendix are still valid, as far as they go.

The model for the proposed design will only change from the base line in its control law for the gimbal motor. Thus equation (5) on page 16 of the appendix will become:

$$T_{Gm} = K_2 \Theta_{RW} - T_{FP} \tag{1}$$

where: T_{FR} = the flex pivot torque

(note a typo lists $\dot{\Theta}_{RW}$ as $\ddot{\Theta}_{RW}$ in the original text.)

$$\text{Now } T_{FP} = K_{FP} \; (\Theta_D - \Theta_T) . \tag{2}$$

By adding equation (1) here to equation (1) of the appendix the result is removal of the dependency on K_{FP} and thus cancellation of the effect of the flex pivot, or spring constant of the torque sensor.

Therefore, if we follow this through to page 17, equations 8-13 remain valid if we set K_{FP} to zero.

The same logic applies to the development in the earlier parts of the appendix that yielded the general system equations. These remain in force, with k (i.e., K_{FP}) set to zero.

The ball bearing shows up as an impulse under T_n, noise torque, to which we must determine the system response.

2.7 System Response

System response to an impulse, as described above, was simulated using the computer program "TF" written at Stanford University. The impulse, applied at T = 0, resulted in a maximum predicted excursion of the telescope from its commanded position of .025 arcsec. This is a very small angle. At this level the system behavior begins to be quantized by the digital-to-analog converters in the gyros. Thus the shape of response shown in Figure 2 is not a realistic image of the true system dynamics. All resemblance to a linear system will begin to erode on this scale. But we do see that the "snapping" of the ball bearing has little effect on the telescope pointing.

The rest of the model behavior is nearly identical to the system described in the preliminary report. The Linear Ball Bearing/Sensor model predicts that the telescope is completely isolated from the gondola. This is different from the earlier system model in which the telescope was explicitly coupled to the gondola behavior by the flex pivot. In practice, the gondola will excite some telescope motion through the nonlinearities in the gimbal.

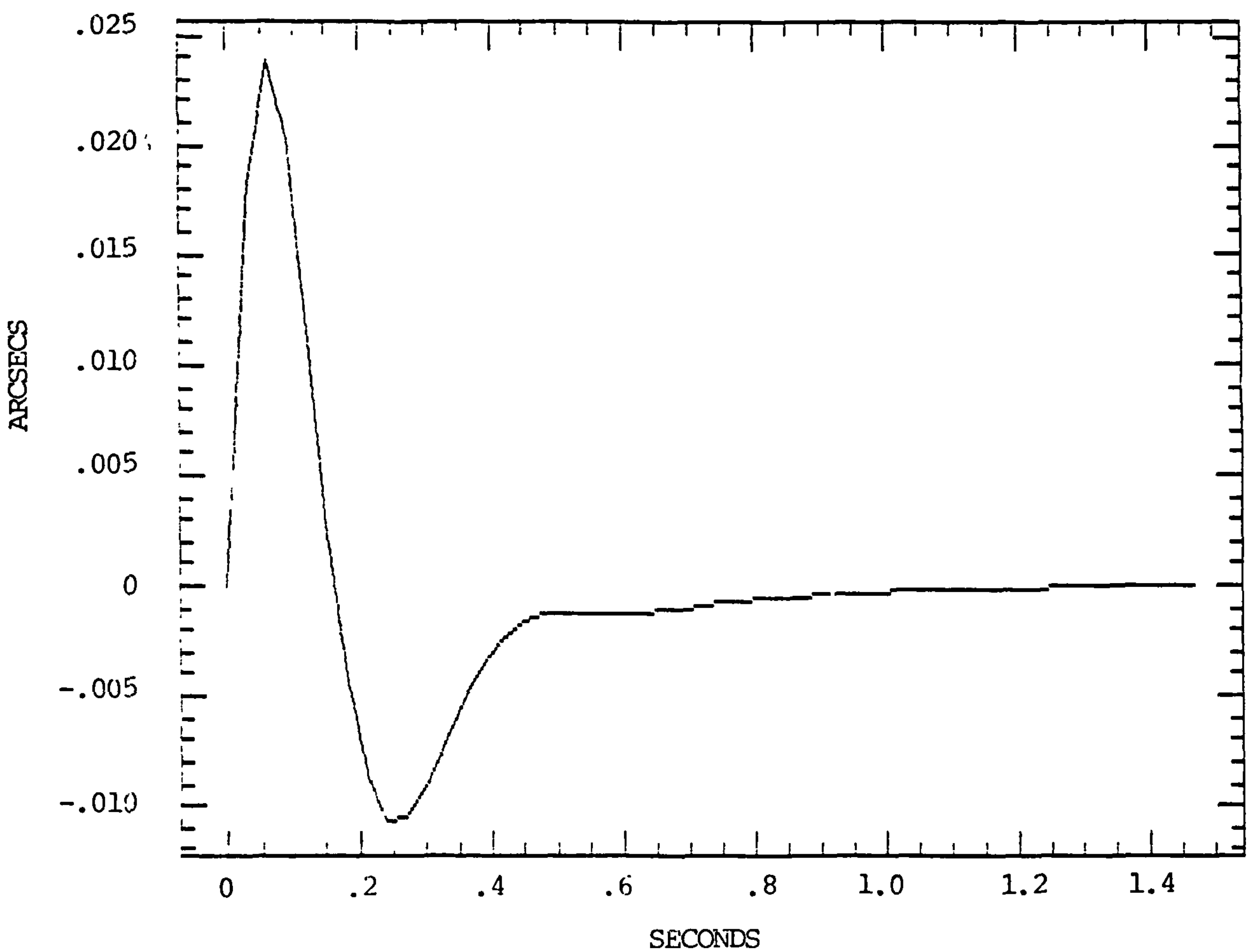

Figure 2 Telescope point response to a $5x10^{-3}$ Nms torque pulse

3.0 RESEARCH PLANNED FOR NEXT REPORTING PERIOD

We plan to continue studies which will lead to determination of system component specifications. A reaction wheel and gimbal motor will be selected and characterized and the system response to these characteristics assessed. Finally, an accurate model of the ball bearing release mechanism must be developed, a goal that will probably require experimentation that is beyond the scope of the present grant but which is under consideration for next year's activity.

APPENDIX A

Pointing Control System Servomechanism Analysis

Glossary of Symbols

Θ_c Angular command (desired pointing) of mirror assembly with respect to inertial space

Θ_m Angular response (actual pointing) of mirror assembly with respect to inertial space

ε_m Angular pointing error of mirror assembly

J_W Moment of inertia of momentum wheel

τ_{TM} Torque developed by momentum wheel torque motor

J_m Moment of inertia of mirror assembly

τ_{ext} External torque applied to mirror assembly

k Spring rate of flex-pivot suspension of mirror assembly [torque units per radian]

T_M Torque developed by ancillary torque motor

Θ_H Angular position of Horseshoe gimbal with respect to local vertical

J_H Moment of inertia of Horseshoe gimbal

ω_H Frequency of angular vibration of Horseshoe gimbal [rad/sec]

S Laplace operator

$\dot{\Theta}_W$ Angular velocity of momentum wheel with respect to inertial space

K' Ancillary torque motor conversion gain [torque units per rad/sec]

AK_τ Amplifier-Torque motor constant [torque units per radian]

T_1 Lead time constant of lead/lag network

T_2 Lag time constant of lead/lag network

$\tau_{applied}$ Total systemic torque applied to the pendulous Horseshoe gimbal (reaction of ancillary torque motor and flex-pivot)

τ_ν Torque Noise (bearing torque noise, motor cogging, etc.)

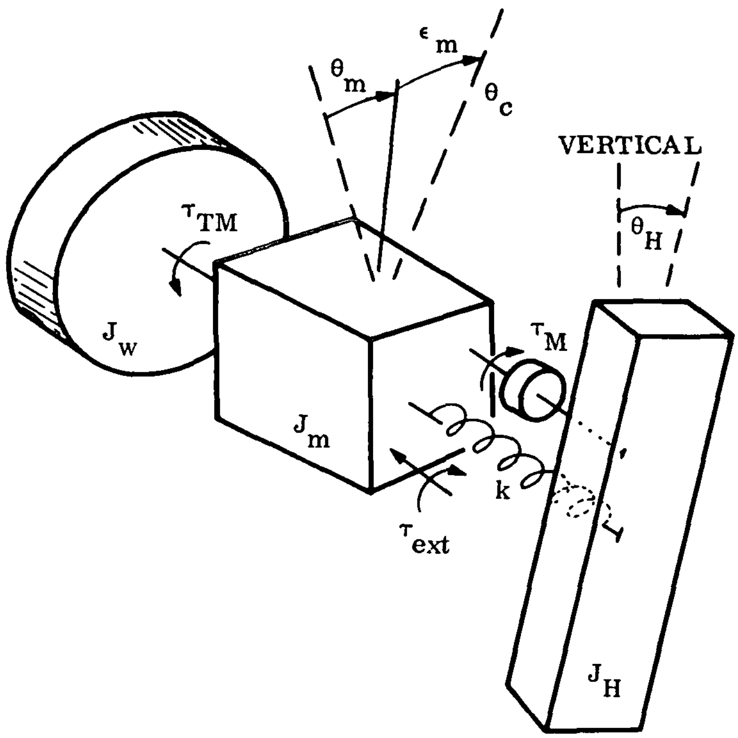

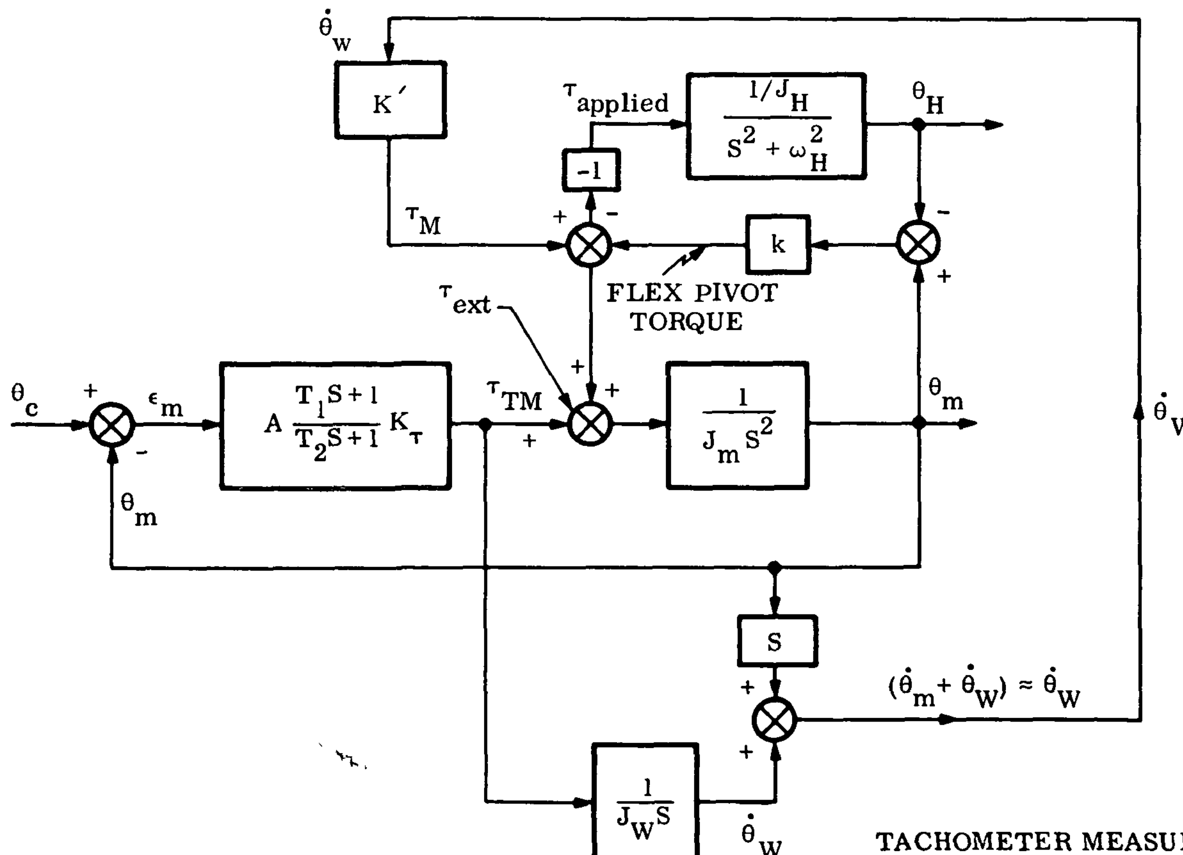

TACHOMETER MEASURE OF
MOMENTUM WHEEL SPEED

System Dynamics Equation is:

$$\begin{bmatrix} \left[J_m S^2 + \frac{T_1 S+1}{T_2 S+1} AK_\tau \left(1 + \frac{K'}{J_W S}\right) + k\right] & -k \\ -\left[k + \frac{T_1 S+1}{T_2 S+1} AK_\tau \frac{K'}{J_W S}\right] & \left[\left(S^2+\omega_H^2\right) J_H + k\right] \end{bmatrix} \begin{Bmatrix} \Theta_m \\ \Theta_H \end{Bmatrix} =$$

$$\begin{Bmatrix} \frac{T_1 S+1}{T_2 S+1} AK_\tau \left(1+\frac{K'}{J_W S}\right)\Theta_c + \tau_{ext} \\ -\frac{T_1 S+1}{T_2 S+1} AK_\tau \frac{K'}{J_W S}\,\Theta_c \end{Bmatrix}$$

Determinant is:

$$\Delta(S) = \frac{1}{S}\left\{ J_m J_H S^5 + \left(J_m J_H \omega_H^2 + J_m k + J_H k\right) S^3 + \frac{T_1 S+1}{T_2 S+1} AK_\tau \left[\left(S^2+\omega_H^2\right)\left(J_H S + \frac{K' J_H}{J_W}\right) + kS\right] + \omega_H^2 J_H k S \right\}$$

which can be recast in form of:

$$\Delta(S) = \frac{1}{S(T_2 S+1)} \left\{K_6 S^6 + K_5 S^5 + K_4 S^4 + K_3 S^3 + K_2 S^2 + K_1 S + K_0\right\}$$

Stable!

Full System Response to Pointing Command

$$\Theta_m = \frac{\begin{vmatrix} \frac{T_1S+1}{T_2S+1} AK_\tau\left(1+\frac{K'}{J_WS}\right)\Theta_c + \tau_{ext} & -k \\ -\frac{T_1S+1}{T_2S+1} AK_\tau \frac{K'}{J_WS}\Theta_c & \left[(S^2+\omega_H^2)J_H+k\right] \end{vmatrix}}{\Delta(S)}$$

or

$$\Theta_m = \frac{1}{\Delta(S)}\left\{\left[(S^2+\omega_H^2)\, J_H\, \frac{T_1S+1}{T_2S+1} AK_\tau \left(1+\frac{K'}{J_WS}\right) + k\frac{T_1S+1}{T_2S+1} AK_\tau\right]\Theta_c + \left[\left(S^2+\omega_H^2\right)J_H+k\right]\tau_{ext}\right\}$$

Final value of mirror pointing is:

$$\Theta_m\Big|_{s.s.} = \lim_{S\to o} S\Theta_m(S) = \lim_{S\to o} \frac{1}{\Delta(o)}\left\{\left[\omega_H^2J_HAK_\tau\left(1+\frac{K'}{J_WS}\right) + kAK_\tau\right]\Theta_c + \left[\omega_H^2J_H+k\right]\tau_{ext}\right\}$$

or

$$\Theta_m\Big|_{s.s.} = \lim_{S\to o} \frac{1}{\omega_H^2 \frac{K'J_H}{J_W} AK_\tau} \left\{ \left[\omega_H^2 J_H AK_\tau \left(S + \frac{K'}{J_W}\right) + kAK_\tau S\right]\Theta_c + \left[\omega_H^2 J_H + k\right] S\, \tau_{ext} \right\}$$

$$= \frac{1}{\omega_H^2 \frac{K'J_H}{J_W} AK_\tau} \left\{ \omega_H^2 \frac{K'J_H}{J_W} AK_\tau \right\} \Theta_c$$

$$= \Theta_c$$

with zero final error even with torsional flex-pivots, external torque, and disturbing horseshoe-motion coupling.

FREQUENCY DOMAIN ERROR ANALYSIS

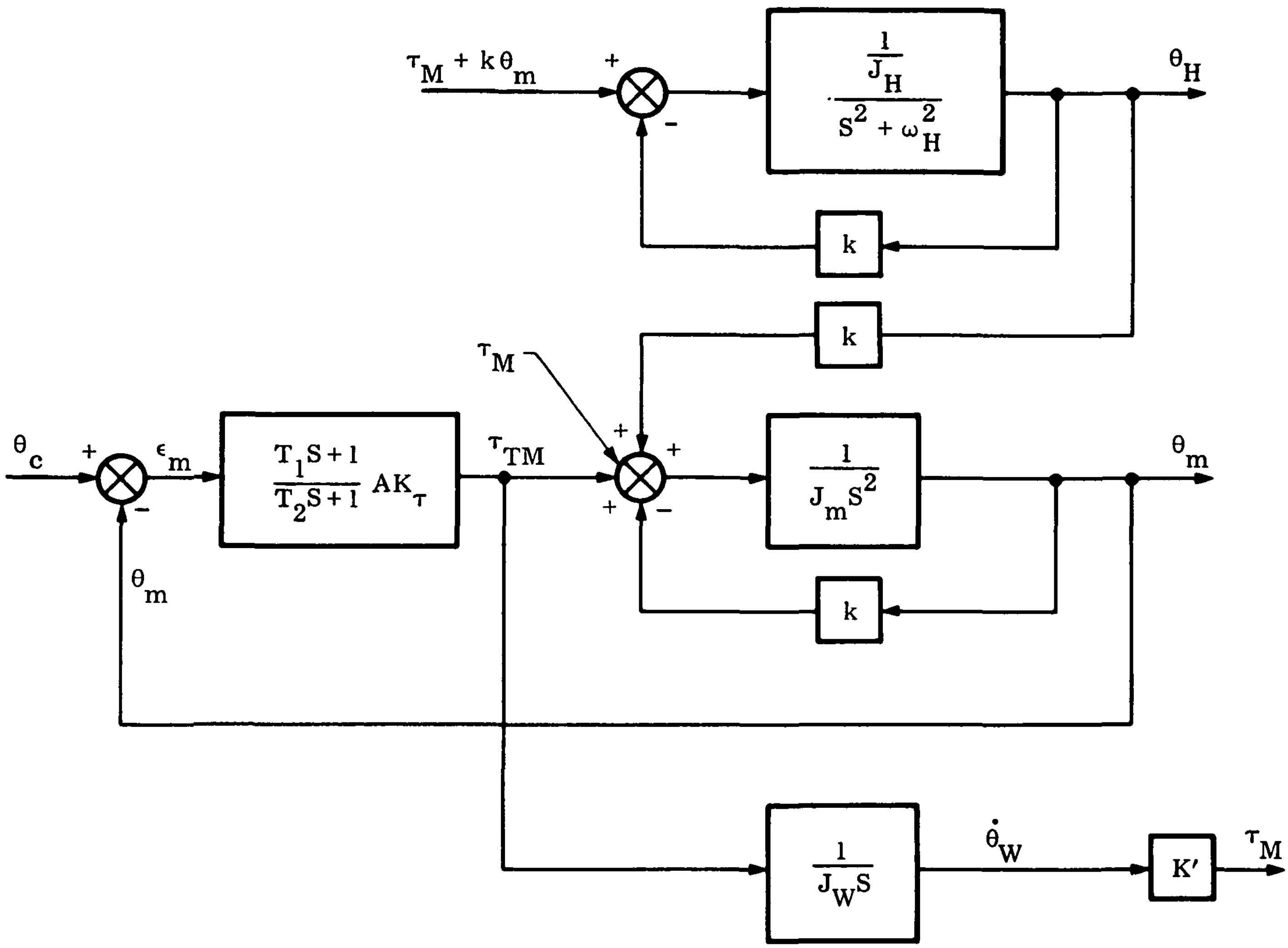

Mirror spectral sensitivity to Horseshoe Gimbal motion is given by:

$$\frac{\Theta_m}{\Theta_H} = \frac{\left(k \frac{J_W}{J_m}\right)\left(T_2 S+1\right) S}{K_4 S^4 + K_3 S^3 + K_2 S^2 + K_1 S + K_0}$$

where

$$K_4 = T_2 J_W$$

$$K_3 = J_W$$

$$K_2 = \left(\frac{J_W}{J_M} kT_2 + \frac{J_W}{J_m} AK_\tau T_1\right)$$

$$K_1 = \left(\frac{J_W}{J_m} k + \frac{AK_\tau K'}{J_m} T_1 + \frac{J_W}{J_m} AK_\tau\right)$$

$$K_0 = \frac{AK_\tau K'}{J_m}$$

Note: •Zero at origin reduces steady-state sensitivity to zero.

•Sensitivity at "horseshoe" gimbal frequency is given by above equation

FREQUENCY DOMAIN SKETCH OF SPECTRAL SENSITIVITY

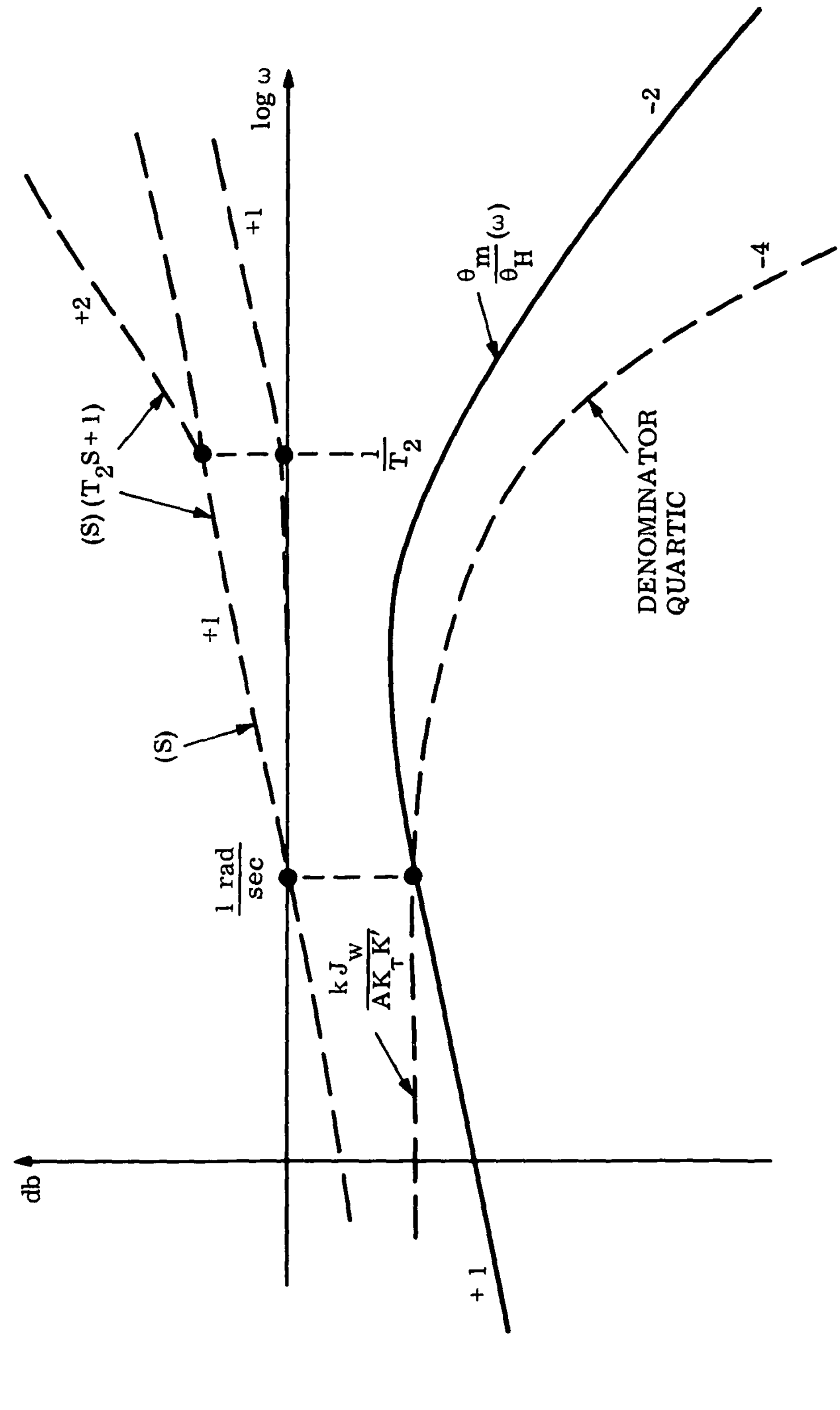

Because "horseshoe" gimbal characteristic frequency, ω_H, is very low, the low frequency asymptote of spectral sensitivity expression may be used:

$$\boxed{\frac{\Theta_m}{\Theta_H} \approx \frac{k\ J_w\ \omega}{A\ K_\tau\ K'}}$$

where $\omega = \sqrt{\omega_H^2 + \frac{k}{J_H}}$, rad/sec

k = flex-pivot constant, [torque units per radian]

J_W = momentum wheel moment of inertia [torque units per radian/sec^2]

AK_τ = amplifier torque motor constant [torque units per radian]

K' = ancillary torque motor conversion gain [torque units per rad/sec.]

J_H = horseshoe moment of inertia [torque units per rad/sec^2]

System Spectral Sensitivity to Torque Noise

$$\frac{\Theta_m}{\tau_\nu}(S) = \frac{1}{\Delta(S)}\left\{(S^2+\omega_H^2)J_H+k\right\}$$

or

$$\frac{\Theta_m}{\tau_\nu}(S) = \frac{S[T_2S+1][S^2+\omega_H^2+\frac{k}{J_H}]J_H}{K_6S^6+K_5S^5+K_4S^4+K_3S^3+K_2S^2+K_1S+K_0}$$

where:

$$K_6 = J_mJ_HT_2$$

$$K_5 = J_mJ_H$$

$$K_4 = [(J_mJ_H\omega_H^2+J_mk+J_Hk)T_2+AK_\tau J_HT_1]$$

$$K_3 = \left[J_mJ_H\omega_H^2+J_mk+J_Hk+AK_\tau J_H+AK_\tau T_1\frac{K'J_H}{J_w}\right]$$

$$K_2 = \left[AK_\tau\frac{K'J_H}{J_W} + AK_\tau(\omega_H^2J_H+k)T_1+\omega_H^2J_HkT_2\right]$$

$$K_1 = \left[AK_\tau(\omega_H^2J_H+k)+AK_\tau\omega_H^2T_1\frac{K'J_H}{J_w} + \omega_H^2J_Hk\right]$$

$$K_0 = AK_\tau\omega_H^2\frac{K'J_H}{J_w}$$

SPECTRAL TORQUE-NOISE SENSITIVITY

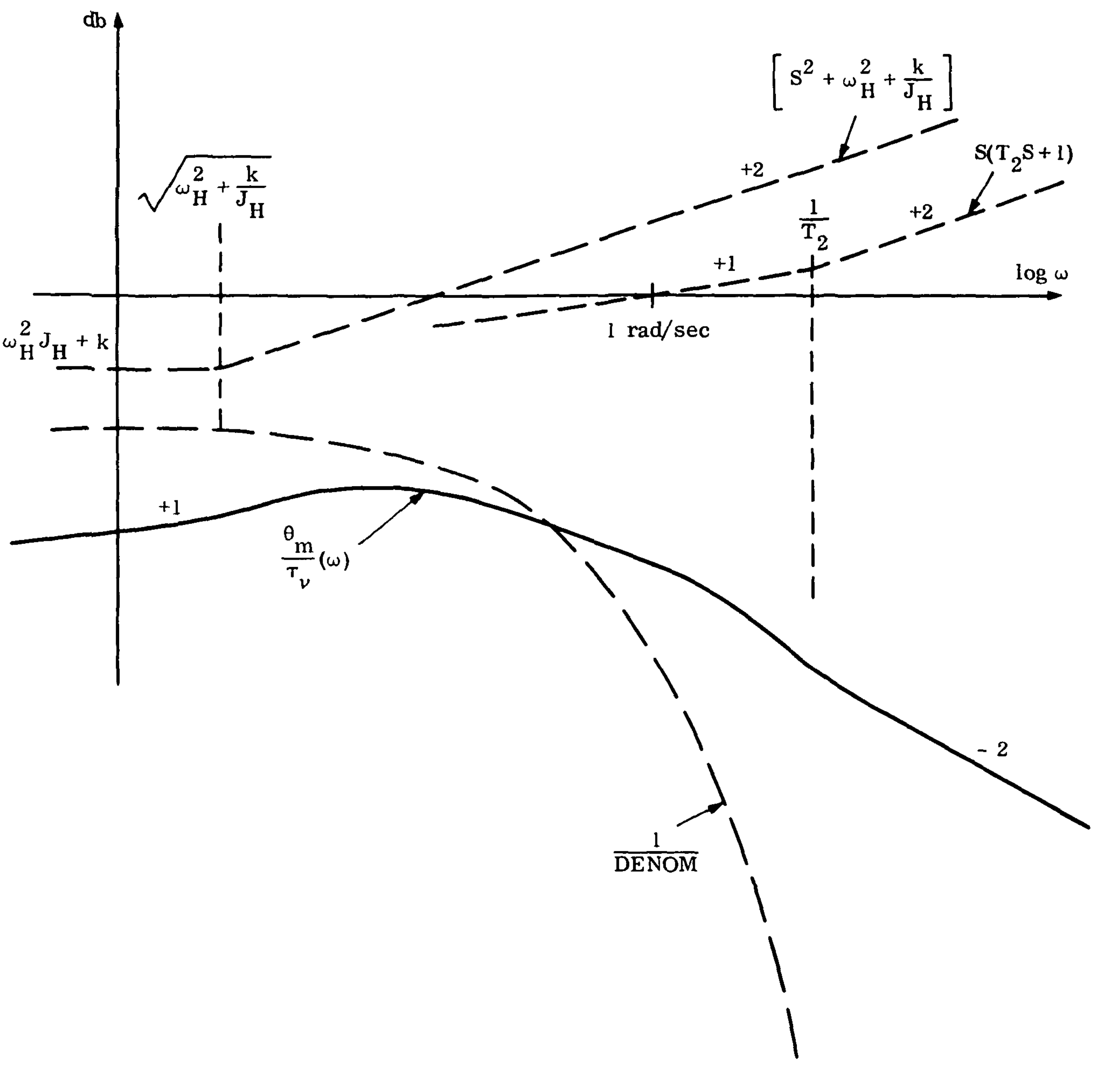

The <u>low</u> <u>frequency</u> asymptote may be approximated by:

$$\frac{\Theta_m}{\tau_\nu} \approx \frac{\left(\omega_H^2+\frac{k}{J_H}\right)J_H}{AK_\tau \omega_H^2 \frac{K' J_H}{J_W}}\ \omega_\nu$$

(low freq.)

$$\approx \frac{\left(\omega_H^2 + \frac{k}{J_H}\right)J_W}{AK_\tau \omega_H^2\ K'}\ \omega_\nu$$

$$\approx \frac{J_W}{AK_\tau K'}\ \omega_\nu$$

<u>where</u> ω_ν is the circular frequency of the torque-noise in rad/sec.

Generic Control

The controlled system can be written as:

$$\ddot{X}_T = -K_{FP}/J_T\ X_T + T_c/J_T + \frac{X_c\ K_{FC}}{J_T} \tag{1}$$

where X_T is the angle being controlled

K_{FP} is a spring constant

J_T is an inertia

T_c is the control torque

X_c is the command input

If we select a simple proportional plus rate controller we have:

$$T_c = -K_g\ (\dot{X}_T\ \tau + X_T) \tag{2}$$

where: τ is the zero location of the controller

K_g is the control gain

Combining (2) and (1) and rewriting we get:

$$\ddot{X}_T + \frac{K_g \tau}{J_T}\ \dot{X}_T + \frac{(K_{FP} + K_g)}{J_T}\ X_T = \frac{K_{FP}}{J_T}\ X_c \tag{3}$$

The generic equation for a 2nd order system like this is:

$$\ddot{X} + 2\zeta\omega_n\ \dot{X} + \omega^2_n X = \omega_n^2\ X_c \tag{4}$$

where: ζ is the damping ratio

ω_n is the natural frequancy

If we select ω_n, ζ we can match coefficients between (4) & (3):

$$\frac{K_g + K_{fp}}{J_T} = \omega^2_{n_o} \tag{5}$$

$$\frac{K_g\ \tau}{J_T} = 2\zeta_o\omega_{n_o} \tag{6}$$

In this way we solve for K_g and τ and get our control.

The individual loops are then combined into a system of equations and solved. Some adjustments are made for the ignored coupling.

Elevation Axis Equation.

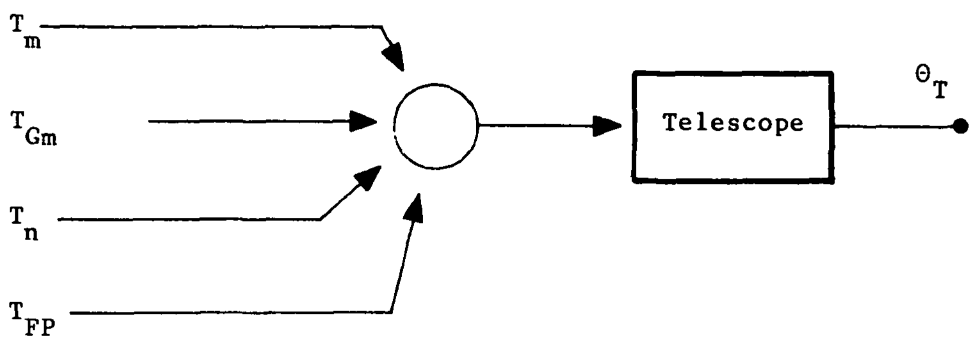

The equation of motion of the telescope is:

$$J_T\ddot{\Theta}_T = K_{FP}(\Theta_g-\Theta_T) + T_{Gm} + T_m + T_n \qquad (1)$$

where: J_T is the telescope inertia

Θ_T is the telescope angular position

K_{FP} is the flex-pivot sprint constant

Θ_g is the gondola's angular position

T_{Gm} is the gimbal motor torque

T_m is the reaction wheel motor

T_n is noise torque

The equation of motion for the gondola is

$$J_g\ddot{\Theta}_g = K_{Fp}(\Theta_T-\Theta_g) - T_{Gm} - \omega_p^2 J_g\Theta_g \qquad (2)$$

where: ω_p is the compound pendulum natural frequency.

Elevation Axis Equation (continued):

Equation of motion of the Reaction Wheel is:

$$J_{r\omega}\,\ddot{\Theta}_{R\omega} = -T_m \tag{3}$$

The control law states:

$$T_m = k_1 \frac{(\tau_1 S+1)}{(\tau_2 S+1)} \tag{4}$$

&

$$T_{Gm} = K_2 \ddot{\Theta}_{R\omega} \tag{5}$$

If we put these equations into state space form as the following:

$$\left.\begin{aligned} X_1 &= \Theta_T \\ X_2 &= \dot{\Theta}_T \\ X_3 &= \Theta_g \\ X_4 &= \dot{\Theta}_g \\ X_5 &= \dot{\Theta}_K \\ X_6 &= \Theta_1 \end{aligned}\right\} \tag{6}$$

where: Θ_1 is used to define a state existing in the control law or:

$$T_m = K_1\,\Theta_1 \tag{7}$$

Elevation Axis Equations:

Eqs. (1), (2), (3) & (4) with eqs. (6) can be put into 6 first order differential equations:

$$\dot{X}_1 = X_2 \tag{8}$$

$$\dot{X}_2 = \frac{1}{J_T}\left[-K_{Fp} X_1 + K_{Fp} X_3 - K_2 X_5 + K_1 X_6 + T_n\right] \tag{9}$$

$$\dot{X}_3 = X_4 \tag{10}$$

$$\dot{X}_4 = \frac{1}{J_g}\left[K_{Fp} X_1 - X_3 (K_{Fp} + \omega_p^2 J_g) + K_2 X_5\right] \tag{11}$$

$$\dot{X}_5 = -\frac{K_1}{J_{F\omega}} X_6 \tag{12}$$

$$\dot{X}_6 = \frac{1}{\tau_2}\left[-X_1 - \tau_2 X_2 - X_6 + X_6\right] \tag{13}$$

Where: X_6 is the commanded signal for the telescope. These equations can be placed in matrix form as

$$\underline{\dot{X}} = [A]\underline{X} + [B]\underline{u} \tag{14}$$

where: [A] is the matrix of coefficients of the x_i's

$$\underline{u} = \begin{bmatrix} x_c \\ T_n \end{bmatrix}$$

$$[B] = \begin{bmatrix} 0 & 0 \\ 0 & \frac{1}{J_T} \\ 0 & 0 \\ 0 & 0 \\ 0 & 0 \\ \frac{1}{\tau_2} & 0 \end{bmatrix}$$

In this form the system was run through a program called "TF" (Transfer Function) written at Stanford University to generate system responses.